

Status of PHOKHARA *

Agnieszka Grzebińska ^a, Henryk Czyż ^b and Agnieszka Wapienik ^b

^aInstitute of Nuclear Physics Polish Academy of Sciences, PL-31342 Cracow, Poland

^bInstitute of Physics, University of Silesia, PL-40007 Katowice, Poland

A review of the status of the Monte Carlo event generator PHOKHARA, developed for experiments using the radiative return method. The four-pion production in electron-positron annihilation and in τ -lepton decays and the narrow resonances studies are described.

1. Introduction

The basis of the radiative return method, proposed in [1], is an observation that one can extract the hadronic cross section ($e^+e^- \rightarrow hadrons$) from the measurement of the cross section of the reaction $e^+e^- \rightarrow hadrons + photons$, where the photons are emitted from the initial leptons. This is possible due to the factorization $d\sigma(e^+e^- \rightarrow hadrons + \gamma_{ISR}) = H(Q^2, \theta_\gamma) d\sigma(e^+e^- \rightarrow hadrons)(s = Q^2)$, where the function H is fully calculable within QED and Q^2 is the invariant mass of the hadronic system.

The radiative return method has been used by meson factories DAPHNE, BaBar and BELLE and allows for the measurement of the hadronic cross section from the nominal energy of these experiments down to the production threshold.

The traditional way of measuring of the hadronic cross section via the energy scan needs dedicated experiments, while using the radiative return one can profit from the existing meson factories. The smaller cross section of the radiative process (by a factor of α/π as compared to the process without photons emission) has to be compensated by higher luminosities of factories.

To obtain the hadronic cross section using the radiative return method in a realistic experimental situation, one needs a Monte Carlo event generator of the measured process. To provide such a tool to the experimental groups PHOKHARA event generator was constructed. The construc-

tion of the PHOKHARA event generator started from the EVA [2,3] generator, where structure function method was used to model multi-photon emission. The physical accuracy of the program was however far from the demanding experimental accuracy. To meet this ever growing demands, the event generator PHOKHARA [4] was constructed. It is based on the complete calculation of radiative corrections to the next-to-leading order for the ISR emission and relevant next-to-leading order corrections to the final state emission. In this paper the latest updates of the four-pion channels [5] are briefly outlined (Section 2) and preliminary results for the narrow resonances implementation are presented (Section 3).

2. The four-pion production in τ decays and e^+e^- annihilation

The four-pion production in e^+e^- annihilation was implemented in the generator EVA [3] a long time ago and recently it was reanalyzed in [5].

There are altogether four different channels accessible for 4π production:

$$\begin{aligned} e^+e^- &\rightarrow 2\pi^+2\pi^-, \\ e^+e^- &\rightarrow 2\pi^0\pi^+\pi^- \quad (\text{a}), \\ \tau^- &\rightarrow \nu_\tau 2\pi^-\pi^+\pi^0 \quad (\text{b}), \\ \tau^- &\rightarrow \nu_\tau 3\pi^0\pi^-. \end{aligned}$$

Assuming isospin symmetry, the amplitudes of either (a) [6] or (b) [7] are sufficient to determine all four amplitudes.

In EVA and PHOKHARA a choice of [6] was adopted and a function J_μ (symmetric under the interchange of p_1 and p_2 and antisymmetric under the interchange of p^+ and p^-) is used to model

*Work supported in part by EU 6th Framework Programme under contract MRTN-CT-2006-035482 (FLAVIANet).

the two e^+e^- four pion channels:

$$\langle \pi^+ \pi^- \pi_1^0 \pi_2^0 | J_\mu^3 | 0 \rangle = J_\mu(p_1, p_2, p^+, p^-), \quad (1)$$

The other matrix elements: $\langle \pi_1^+ \pi_2^+ \pi_1^- \pi_2^- | J_\mu^3 | 0 \rangle$, $\langle \pi^- \pi_1^0 \pi_2^0 \pi_3^0 | J_\mu^- | 0 \rangle$ and $\langle \pi_1^- \pi_2^- \pi^+ \pi^0 | J_\mu^- | 0 \rangle$ can be expressed as sum of J_μ functions with permuted arguments [6].

For e^+e^- annihilation the current J_μ contains the complete information about the hadronic cross section through

$$\int J_\mu^{em} (J_\nu^{em})^* d\bar{\Phi}_n(Q; q_1, \dots, q_n) = \frac{1}{6\pi} (Q_\mu Q_\nu - g_{\mu\nu} Q^2) R(Q^2), \quad (2)$$

where $R(Q^2) = \sigma(e^+e^- \rightarrow \text{hadrons})(Q^2)/\sigma_{\text{point}}$. Similarly for τ decay we have

$$\int J_\mu^- J_\nu^{*-} d\bar{\Phi}_n(Q; q_1, \dots, q_n) = \frac{1}{3\pi} (Q_\mu Q_\nu - g_{\mu\nu} Q^2) R^\tau(Q^2) \quad (3)$$

where R^τ can be obtained from the differential τ decay rates.

From the isospin relations between the matrix elements of the four pion hadronic current one obtains the relations between τ decay rates and e^+e^- annihilation cross sections

$$\begin{aligned} R^\tau(-000) &= \frac{1}{2} R(+ + - -) \\ R^\tau(- - + 0) &= \frac{1}{2} R(+ + - -) \\ &+ R(+ - 0 0). \end{aligned} \quad (4)$$

They allow for direct tests of the isospin symmetry provided all R functions were measured.

The latest (still preliminary) accurate measurement (by means of the radiative return method) by BaBar [8] of the $2\pi^0\pi^+\pi^-$ mode complemented the precise e^+e^- data sets by CMD2 [9], SND [10] and BaBar [11]. Together with the τ data from ALEPH [12] and CLEO [13] it allows for model independent isospin symmetry tests.

Combining the results from BaBar [11,8] and using relations between τ and e^+e^- Eq.(4), we obtain predictions for the τ spectral functions v (related directly to R^τ [5]). We use normalization of the spectral functions chosen by ALEPH [12].

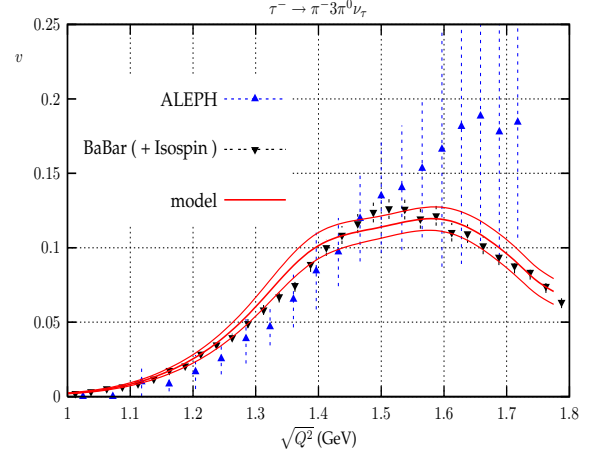


Figure 1. The spectral function of the $\tau^- \rightarrow 3\pi^0\pi^-\nu_\tau$ decay mode. ALEPH [12] data versus predictions from BaBar [11,8] and the model [5].

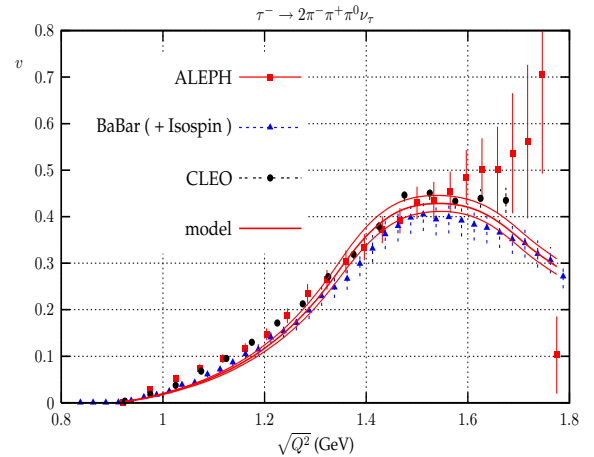


Figure 2. The spectral function of the $\tau^- \rightarrow 2\pi^-\pi^+\pi^0\nu_\tau$ decay mode. ALEPH [12] and CLEO [13] data versus predictions from BaBar [11,8] and the model [5].

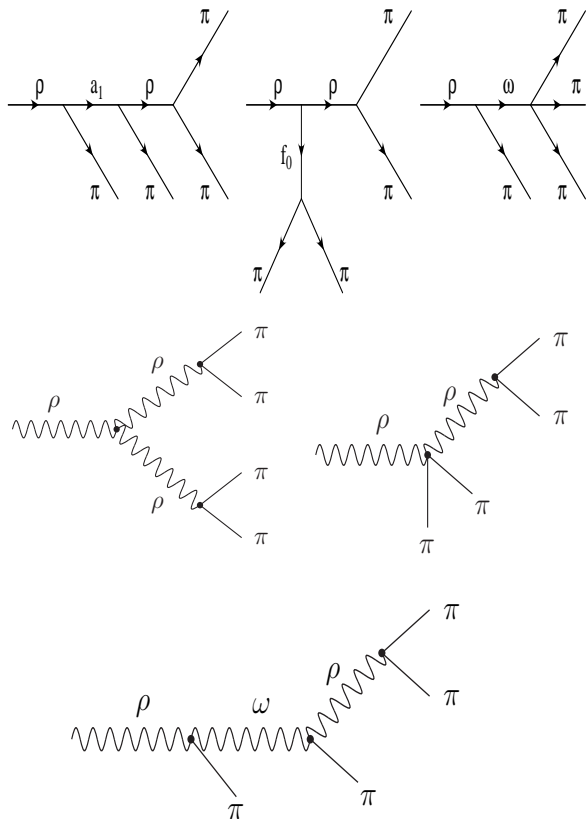


Figure 3. Diagrams contributing to the hadronic current in [3] (upper) and the new contributions from ρ mesons (middle) and the omega (lower).

As shown in Fig.1 and Fig.2 there is a good agreement between the spectral functions predicted from the BaBar data and the isospin symmetry and the ones measured by ALEPH and CLEO. One observes systematic shifts which are however well contained within current error bars and it is not possible to claim an observation of the isospin symmetry violation.

Old 4π model adopted from [14] and used in [3] cannot reproduce new and more accurate data. The update to the model has been constructed in [5]. Amplitudes used in the new model are schematically depicted in Fig.3. The upper diagrams show old contributions from [3], the middle diagrams represent newly added contribu-

	$\text{Br}(\tau^- \rightarrow \nu_\tau 2\pi^- \pi^+ \pi^0)$
PDG [15]	$(4.46 \pm 0.06)\%$
model	$(4.12 \pm 0.21)\%$
BaBar (CVC)	$(3.98 \pm 0.30)\%$

$\text{Br}(\tau^- \rightarrow \nu_\tau \pi^- \omega (\pi^- \pi^+ \pi^0))$	$\text{Br}(\tau^- \rightarrow \nu_\tau \pi^- 3\pi^0)$
$(1.77 \pm 0.1)\%$	$(1.04 \pm 0.08)\%$
$(1.60 \pm 0.13)\%$	$(1.06 \pm 0.09)\%$
$(1.57 \pm 0.31)\%$	$(1.02 \pm 0.05)\%$

Table 1

Branching ratios of τ decay modes. Comparison between model, experimental data [15] and predictions based on BaBar data [11,8] and isospin symmetry.

tions where the ρ particles are treated as SU(2) gauge bosons and the lower diagram represent new omega contributions, which substitute the last diagram of the first line.

There are following parameters in the model: external masses and widths $m_{\rho'}$, $\Gamma_{\rho'}$, $m_{\rho''}$, $\Gamma_{\rho''}$, $m_{\rho'''}$, $\Gamma_{\rho'''}$, four couplings in each of the a_1 , f_0 and ω parts and one coupling in ρ -part. The parameters were fitted to the existing data. The fit is quite good, with $\chi^2/n_{d.o.f} = 275/287$.

The comparison between new model and the data from ALEPH, CLEO and BaBar are shown in Fig.1 and Fig.2. The upper and lower curves represent error bars.

It is interesting to compare also the τ branching ratios from the PDG [15], the new model predictions and the direct predictions from BaBar data using isospin symmetry. The results are collected in Table 1. They are in agreement within current error bars. One can observe about two sigma difference between PDG and BaBar data for $\text{Br}(\tau^- \rightarrow \nu_\tau 2\pi^- \pi^+ \pi^0)$. Better precision BaBar data, expected after the preliminary results [8] are published, might shed light on the isospin violation in the four pion e^+e^- production and τ decays.

3. The narrow resonances J/ψ and $\psi(2S)$ in PHOKHARA

The implementation the narrow resonances J/ψ and $\psi(2S)$ to the PHOKHARA event generator is the latest update of this program. The final results will be presented soon and in this paper we present the preliminary results.

Contributions from two narrow resonances

$$J/\psi \rightarrow m = 3096.916 \text{ MeV}, \Gamma = 93.4 \text{ keV}$$

$$\psi(2S) \rightarrow m = 3686.093 \text{ MeV}, \Gamma = 337 \text{ keV},$$

to the final states:

$\pi^+\pi^-$, $\mu^+\mu^-$, K^+K^- and $K^0\bar{K}^0$ were implemented in PHOKHARA.

In general one has three types of contributions to the production amplitude at the narrow resonance (Fig.4): one-photon continuum, one-photon decays and three-gluon decays. The last amplitude contributes only to the K^+K^- and $K^0\bar{K}^0$ production.

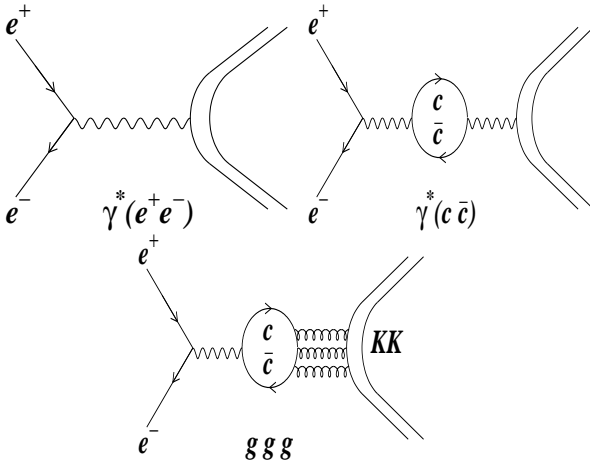


Figure 4. The Feynman diagrams of $e^+e^- \rightarrow \mu^+\mu^-, \pi^+, \pi^-, KK$ at charmonium resonance, the one-photon continuum process, the one-photon decays and the three-gluon decays (only for kaons).

For reliable predictions of the $\pi^+\pi^-$ and KK

production good models of electromagnetic pion and kaon form factors are needed. The form factors used in the public version of PHOKHARA 6.0 were taken from [16]. The CLEO-c measurement [17] and results of the investigations in [18] and [19] were not accounted for in [16]. As a result, the values of form factors taken from [16] at the J/ψ and $\psi(2S)$ are much smaller than the ones obtained in [17,18,19] and new investigations were necessary.

For the pion form factor we keep the structure of the model from [16]:

$$F_\pi(s) = \left[\sum_{n=0}^N c_{\rho_n} BW_n(s) \right]_{fit} + \left[\sum_{n=N+1}^{\infty} c_{\rho_n} BW_n(s) \right]_{dual-QCD_{N_c=\infty}}, \quad (5)$$

where firsts $N-1$ couplings are fitted (c_N is calculated). We perform the fit taking into account the experimental data not accounted for in [16]. For kaons, unlike in [16], we use infinite towers of resonances for ρ , ω and ϕ (see [20] for more details). The results of the fits are summarized in Fig.5. For pions we considered two versions of the model, where the Breit-Wigner function was taken at tree level [21] - Kühn-SantaMaria (KS) model and where it was taken with pion loop corrections [22] - Gounaris-Sakurai (GS) model. For kaons we also considered two versions of the model, constrained and unconstrained (see [16] for the details).

One has to remember that due to the finite detector resolution one never observes the true distribution of the events but its convolution with the detector resolution function. This is extremely important for studies of the narrow resonances, where typical energy resolution is much bigger than a width of a resonance. Fig.6 shows the differential cross section of the process $e^+e^- \rightarrow J/\psi\gamma \rightarrow \pi^+\pi^-\gamma(\gamma)$ with true distribution of the events (solid line) and the realistic differential cross section obtained by smearing with the Gaussian distribution with the 14.5 MeV standard deviation (taken from [24]).

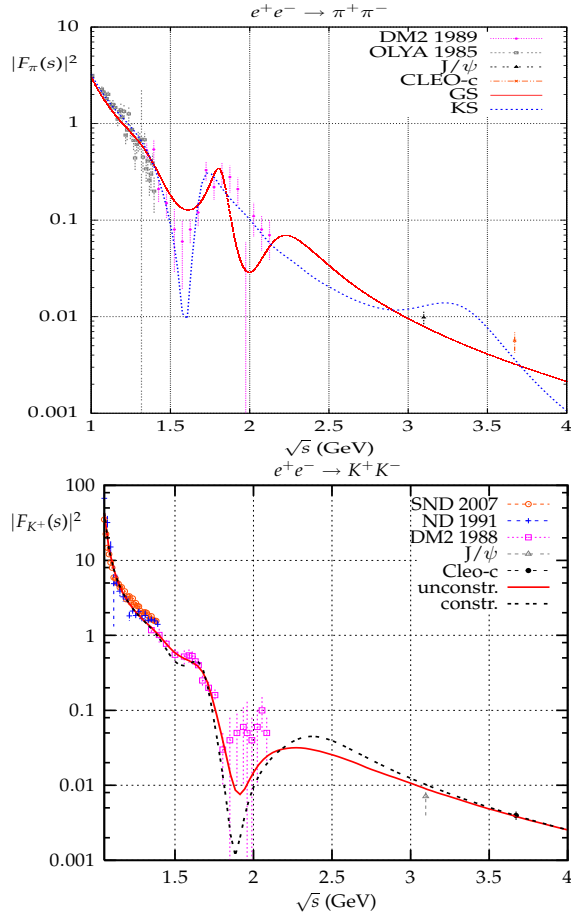


Figure 5. The experimental data [17,23] compared to the model fits results. The form factor at J/ψ is from [19] (theoretical extraction).

We investigated also the role of the FSR radiation (at next to leading order) on the radiative return cross sections in the vicinity of the narrow resonances. In Fig.7 we show the results for two pion final state. Relatively big corrections to the differential Q^2 distribution, coming from FSR (IFSNLO=FSRNLO+ISRNLO) are observed as compared to the ISRNLO only, even if the integrated cross sections differ only by about 2%.

4. Conclusions

The present status of the PHOKHARA event generator was described. The four-pion channels

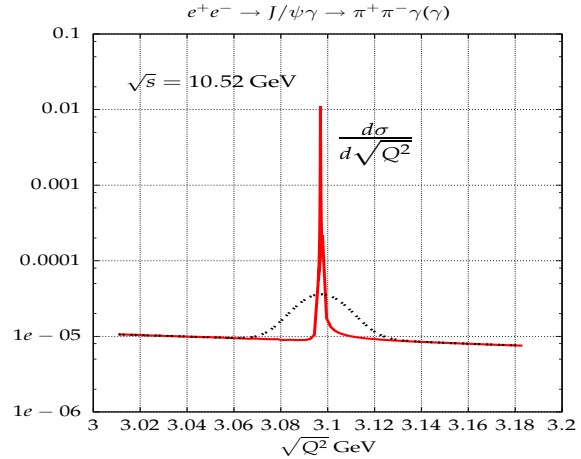


Figure 6. Differential cross section for $\sqrt{s} = 10.52$ GeV of the process $e^+e^- \rightarrow J/\psi\gamma \rightarrow \pi^+\pi^-\gamma(\gamma)$ without (solid line) and with the detector smearing effect.

reanalysis and the latest upgrade of the generator, implementation of narrow resonances, were presented.

REFERENCES

1. Min-Shih Chen and P. M. Zerwas, Phys. Rev. D **11** (1975) 58.
2. S. Binner, J. H. Kühn and K. Melnikov, Phys. Lett. B **459** (1999) 279 [hep-ph/9902399].
3. H. Czyż and J. H. Kühn, Eur. Phys. J. C **18**, 497 (2001) [arXiv:hep-ph/0008262].
4. G. Rodrigo, H. Czyż, J.H. Kühn and M. Szopa, Eur. Phys. J. C **24**, 71 (2002) [arXiv:hep-ph/0112184]; H. Czyż, A. Grzelinska, J. H. Kuhn and G. Rodrigo, Eur. Phys. J. C **27**, 563 (2003) [arXiv:hep-ph/0212225]; Eur. Phys. J. C **33**, 333 (2004) [arXiv:hep-ph/0308312]; Eur. Phys. J. C **39**, 411 (2005) [arXiv:hep-ph/0404078]; Eur. Phys. J. C **47**, 617 (2006) [arXiv:hep-ph/0512180]; H. Czyż, J. H. Kühn, E. Nowak and G. Rodrigo, Eur. Phys. J. C **35**, 527 (2004) [arXiv:hep-ph/0403062]; H. Czyż,

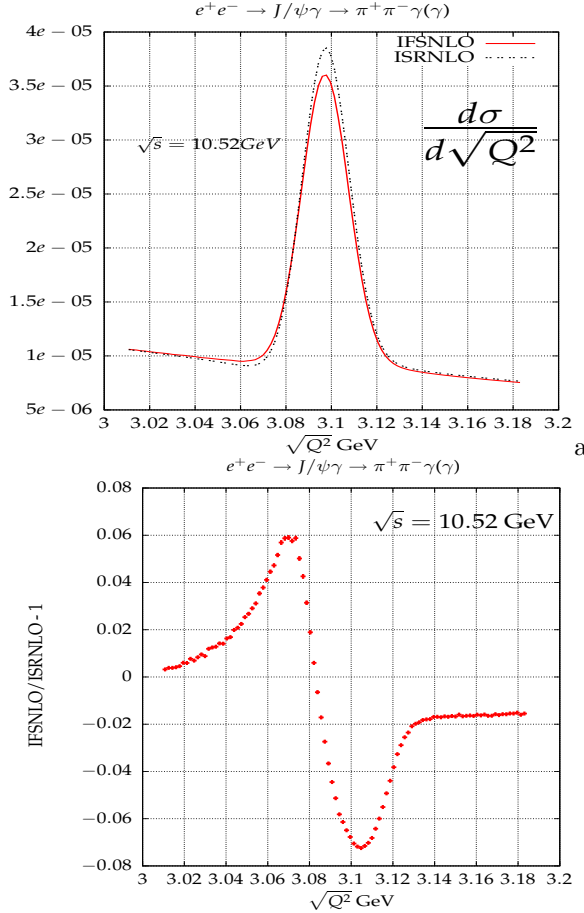


Figure 7. The size of the next-to-leading FSR correction (IFSNLO) compared with the next-to-leading ISR correction (ISRNLO). Detector smearing effect are taken into account.

A. Grzelińska and J. H. Kühn, Phys. Lett. B **611**, 116 (2005) [arXiv:hep-ph/0412239]; Phys. Rev. D **75**, 074026 (2007) [arXiv:hep-ph/0702122].

5. H. Czyż, J. H. Kühn and A. Wapienik, Phys. Rev. D **77**, 114005 (2008) [arXiv:0804.0359[hep-ph]].

6. J. H. Kuhn, Nucl. Phys. Proc. Suppl. **76**, 21 (1999) [arXiv:hep-ph/9812399];

7. G. Ecker and R. Unterdorfer, Eur. Phys. J. C **24**, 535 (2002) [arXiv:hep-ph/0203075];

8. A. Petzold, presentation at EPS Confer-

ence, Manchester 2007; V. P. Druzhinin, arXiv:0710.3455 [hep-ex].

9. R. R. Akhmetshin *et al.* [CMD-2 Collaboration], Phys. Lett. B **595**, 101 (2004) [arXiv:hep-ex/0404019].

10. M. N. Achasov *et al.*, J. Exp. Theor. Phys. **96**, 789 (2003) [Zh. Eksp. Teor. Fiz. **123**, 899 (2003)].

11. B. Aubert *et al.* [BABAR Collaboration], Phys. Rev. D **71**, 052001 (2005) [arXiv:hep-ex/0502025].

12. S. Schael *et al.* [ALEPH Collaboration], Phys. Rept. **421**, 191 (2005) [arXiv:hep-ex/0506072].

13. K. W. Edwards *et al.* [CLEO Collaboration], Phys. Rev. D **61**, 072003 (2000) [arXiv:hep-ex/9908024].

14. R. Decker, M. Finkemeier, P. Heiliger and H. H. Jonsson, Z. Phys. C **70**, 247 (1996) [arXiv:hep-ph/9410260];

15. W. M. Yao *et al.* [Particle Data Group], J. Phys. G **33**, 1 (2006).

16. C. Bruch, A. Khodjamirian and J.H. Kühn, Eur. Phys. J. C **39** (2005) 41, [hep-ph/0409080].

17. T. K. Pedlar *et al.* [CLEO Collaboration], Phys. Rev. Lett. **95**, 261803 (2005) [arXiv:hep-ex/0510005].

18. J. Milana, S. Nussinov and M. G. Olsson, Phys. Rev. Lett. **71**, 2533 (1993) [arXiv:hep-ph/9307233].

19. K. K. Seth, Phys. Rev. D **75** (2007) 017301 [hep-ex/0701005].

20. H. Czyż *et al.* paper in preparation.

21. J. H. Kuhn and A. Santamaria, Z. Phys. C **48**, 445 (1990).

22. G. J. Gounaris and J. J. Sakurai, Phys. Rev. Lett. **21**, 244 (1968).

23. L. M. Barkov *et al.*, Nucl. Phys. B **256** (1985) 365; D. Bisello *et al.* [DM2 Collaboration], Z. Phys. C **39**, 13 (1988); D. Bisello *et al.* [DM2 Collaboration], Phys. Lett. B **220**, 321 (1989); S. I. Dolinsky *et al.*, Phys. Rept. **202**, 99 (1991); M. N. Achasov *et al.*, Phys. Rev. D **76**, 072012 (2007) [arXiv:0707.2279 [hep-ex]].

24. B. Aubert *et al.* [BABAR Collaboration], Phys. Rev. D **69**, 011103 (2004) [arXiv:hep-ex/0310027].